The Prototype Ge−H Insertion Reaction of Germylene with Germane. Absolute Rate Constants, Temperature Dependence, RRKM Modeling and the Potential Energy Surface

Rosa Becerra,[†] Sergei E. Boganov,[‡] Mikhail P. Egorov,[‡] Valery I. Faustov,[‡] Oleg M. Nefedov,[‡] and Robin Walsh*[,§]

Contribution from the Instituto de Quimica-Fisica "Rocasolano", C.S.I.C., C/Serrano 119, 28006 Madrid, Spain, the N.D. Zelinsky Institute of Organic Chemistry, Russian Academy of Sciences, Leninsky Prospekt 47, 117913 Moscow, Russian Federation, and the Department of Chemistry, University of Reading, Whiteknights, P.O. Box 224, Reading RG6 6AD, UK

Received September 9, 1998

Abstract: Time-resolved studies of germylene, GeH_2, generated by laser flash photolysis of 3,4-dimethylgermacyclopentene-3, have been carried out to obtain rate constants for its bimolecular reaction with monogermane, GeH_4. The reaction was studied in the gas phase over the pressure range 1−100 Torr, with SF_6 as bath gas, at five temperatures in the range 292−520 K. The reaction of GeH_2 with GeH_4 to form digermane, Ge_2H_6, is pressure dependent, consistent with a third-body assisted association reaction. The high-pressure rate constants, obtained by extrapolation, gave the following Arrhenius equation: $\log(k^\infty/\mathrm{cm^3\ molecule^{-1}\ s^{-1}}) = (-11.17 \pm 0.10) + (5.2 \pm 0.7\ \mathrm{kJ\ mol^{-1}})/RT\ \ln 10$. These Arrhenius parameters are consistent with a moderately fast reaction occurring at approximately one-fifth of the collision rate. RRKM modeling, based on a variational transition state, used in combination with a weak collisional deactivation model, gave good fits to the pressure dependent curves, for a suitable choice of the critical energy, E_o, for reverse decomposition of Ge_2H_6. The step size (energy removed in a down collision) was chosen by analogy with the corresponding system for Si_2H_6 (collisional efficiency (β_c) of ca. 0.7 for SF_6). The value obtained for E_o was 155 kJ mol^{-1}. Corrected for thermal energy and combined with the insertion activation energy this gives $\Delta H° = 166$ kJ mol^{-1} for the decomposition of Ge_2H_6. There is no previous experimental determination of this quantity. From it we derive $\Delta H_f^{\circ}(GeH_2) = 237 \pm 12$ kJ mol^{-1}, in reasonable agreement with earlier estimates. From bond dissociation energy values the Divalent State Stabilization Energy (DSSE) of germylene (119 kJ mol^{-1}) is larger than that of silylene (94 k J mol^{-1}). *Ab initio* calculations at the correlated level reveal the presence of two weak complexes (local energy minima) on the potential energy surface corresponding to either direct or inverted geometry of the inserting germylene fragment. Surprisingly, the latter is the lower in energy, lying 25 kJ mol^{-1} below the unassociated reactants. These complexes rearrange to digermane with very low barriers. The implications of these findings and the nature of the insertion process are discussed.

Introduction

The reaction between germylene, GeH_2, and monogermane, GeH_4, *viz.*

$$GeH_2 + GeH_4 \rightarrow Ge_2H_6 \qquad (1)$$

may reasonably be considered the prototype Ge−H insertion process of germanium hydride chemistry. GeH_2 is known to be important in the chemical vapor deposition of semiconductor germanium,[1,2] and is the key intermediate in the breakdown mechanism of GeH_4.[3] Reaction 1 is known to occur when GeH_2 is made via recoil Ge atoms generated in the neutron bombardment in GeH_4.[4] It is reasonable to assume that reaction 1 is the likely second step in any process leading to the generation of Ge_2H_6 from GeH_4. We have recently obtained the first direct experimental rate constants[5,6] for reactions of GeH_2 in the gas phase. Our results[5] confirm that while GeH_2 is a very reactive intermediate and shows a similar pattern of reactivity to that of SiH_2, the rate constants of its reactions are less than those of SiH_2. We have also found,[6] in the first temperature variation study, that GeH_2 inserts into Ge−H bonds with a negative activation energy that is greater (*i.e.* more negative) than the analogous SiH_2 reaction with an Si−H bond. This indicates that GeH_2 reactions slow more than SiH_2 reactions at high temperatures.

We report here the extension of our germylene studies to the kinetics of reaction 1, for which no previous investigations exist. We also report theoretical, ab initio, calculations of the potential energy surface for which Trinquier[7] has found evidence of intermediate complexes. Because reaction 1 is an association

[†] Instituto "Rocasolano".
[‡] Zelinsky Institute.
[§] University of Reading.

(1) Isobe, C.; Cho, H.; Sewell, J. E. *Surf. Sci.* **1993**, *295*, 117.
(2) Du, W.; Keeling, L. A.; Greenlief, C. M. *J. Vac. Sci. Technol. A* **1994**, *12*, 2281.
(3) Newman, C. G.; Dzarnoski, J.; Ring, M. A.; O'Neal, H. E. *Int. J. Chem. Kinet.* **1980**, *12*, 661.
(4) Gaspar, P. P.; Levy, C. A.; Frost, J. J.; Bock, S. A. *J. Am. Chem. Soc.* **1969**, *91*, 1573.
(5) Becerra, R.; Boganov, S. E.; Egorov, M. P.; Nefedov, O. M.; Walsh, R. *Chem. Phys. Lett.* **1996**, *260*, 433.
(6) Becerra, R.; Boganov, S. E.; Egorov, M. P.; Nefedov, O. M.; Walsh, R. *Mendeleev Commun.* **1997**, 87.
(7) Trinquier, G. *J. Chem. Soc., Faraday Trans.* **1993**, *89*, 775.

10.1021/ja983223m CCC: $15.00
Published on Web 11/20/1998

reaction, it can yield information on the energy released, through an experimental investigation of its pressure dependence combined with theoretical (RRKM) modeling. This forms part of the study described here and leads to a value for ΔH_f° (GeH_2), for which information is sparse. This study parallels our earlier investigation[8] of the reaction,

$$SiH_2 + SiH_4 \rightarrow Si_2H_6 \qquad (2)$$

In our earlier studies,[5,6] the reported rate constants for GeH_2 were all based on the use of 3,4-dimethylgermacyclopentene-3 as photoprecursor. The other potential precursor we used,[5] viz., phenylgermane, while giving clear spectroscopic signals for GeH_2, gave apparent values for rate constants which were ca. 2−4 times too low, depending on reaction partner. To provide further support for validity of our measurements we have briefly investigated the use of mesitylgermane as a further germylene precursor. The results are reported here.

Experimental Section

Rate Measurements. The apparatus, procedures, data acquisition, and analysis method have been described in general[9] and their application to germylene kinetic studies in particular.[5,6] Only essential and brief details are therefore included here. GeH_2 was produced by the 193 nm flash photolysis of 3,4-dimethylgermacyclopentene-3 (DMGCP) or 1,3,5-trimethylphenylgermane (mesitylgermane, $MesGeH_3$) with use of a Coherent Compex 100 exciplex laser. GeH_2 concentrations were monitored in real time by means of a Coherent 699-21 single-mode dye laser pumped by an Innova 90-5 argon ion laser and operating with Rhodamine 6G. Experiments were carried out in a variable-temperature spectrosil quartz vessel with demountable windows[10] which were regularly cleaned. Photolysis laser pulse energies were typically 50−70 mJ with a variation of ±5%. The monitoring laser beam was multipassed up to 36 times through the reaction zone to give an effective path length of up to 1.2 m. The laser wavelength was set by the combined use of a wavemeter (Burleigh WA-20) and reference to a known coincident transition in the visible spectrum of I_2 vapor and was checked at frequent intervals during the experiments.

The monitoring laser beam was tuned to the strong vibration−rotation transition at 17111.31 cm^{-1} (A $^1B_1(0,1,0) \leftarrow$ X $^1A_1(0,0,0)$) band) discovered by us previously.[5] Light signals were measured by a dual photodiode-differential amplifier combination, and signal decays were stored in a transient recorder (Datalab DL 910) interfaced to a BBC microcomputer. This was used to average the decays of typically 5 laser shots (at a repetition rate of 1 or 2 Hz). Signal decays were found to be exponential up to 90% and were fitted by a least-squares procedure to provide values for the first-order rate coefficients, k_{obs}, for removal of GeH_2 in the presence of known partial pressures of GeH_4.

Gas mixtures for photolysis were made up consisting of 2−6 mTorr of precursor (usually DMGCP), variable pressures of GeH_4 between 20 and 1000 mTorr, and inert diluent SF_6 bath gas up to total pressures between 1 and 100 Torr. Pressures were measured with capacitance manometers (MKS Baratron).

The germanium-containing compounds were obtained as follows. DMGCP was prepared as previously described.[5] Mesitylgermane was synthesized in two stages. First mesityltrichlorogermane was made (yield 54%) by reaction of $GeCl_4$ with excess of mesitylmagnesium bromide by analogy with the method of Mironov and Gar.[11] Then mesitylgermane was prepared (yield 83%) by treatment of mesityltrichlorogermane with $LiAlH_4$ in dried diethyl ether by standard procedures.[12] After distillation its purity was ca. 99%. Spectral analyses (IR, NMR) are in agreement with published data.[13] Germane was prepared by the sodium borohydride reduction of germanic acid.[14,15] GeO_2 (Aldrich, 99.998% pure) was dissolved in NaOH solution to which was added the $NaBH_4$. When dissolved this solution was added, dropwise, to stirred glacial acetic acid. The GeH_4 formed was carried from the flask in a stream of N_2, via a −120 °C slush bath to remove CH_3COOH, and into a liquid nitrogen cooled trap. The crude product was trap-to-trap distilled, via the −120 °C trap again, to purify it. Its purity (99%) was checked via IR,[16] which confirmed the removal of all traces of acetic acid.

SF_6 was obtained from ICI and contained no GC detectable impurities.

Ab Initio Calculations. These were carried out in general at two levels of theory.[17] Geometry optimizations, vibrational analyses, and reaction paths were performed at the frozen core, MP2/6-311G(d,p) level. All the structures obtained here were verified, by examination of the frequency matrix, as minima (all frequencies real) or transition states (one imaginary frequency). Energies were corrected to include zero-point vibrational (ZPE) contributions. Final energies were refined at the G2 level.[18] Total energies calculated in G2 theory are effectively those at the QCISD(T)/6-311G+(3df,2pd) level, making certain assumptions about additivity of the corrections and using the geometry taken from the MP2(full)/6-31G(d) optimization with ZPE contributions calculated from frequencies at the HF/6-31G(d) level.[18] Our G2 calculations differ slightly from this in that we used both geometries and frequencies from the MP2/6-311G(d,p) calculation. ZPE corrections were calculated by using the scaling factor 0.9748 recommended for this level.[19] These calculations are denoted subsequently in this paper as G2//MP2/6-311G(d,p).

Because of the unusual nature of the potential surfaces we verified our results by carrying out calculations along the minimum energy paths (intrinsic reaction coordinates, IRC) connecting transition states with local minima. Most of the calculations carried out here were performed with GAUSSIAN 94[20] on the SGI POWER CHALLENGE L supercomputer at the computer center of IOC RAS, Moscow.

Results

Rate Measurements. Prior to investigating reaction 1, preliminary experiments were carried with $MesGeH_3$ as precursor. Excimer laser photolysis of $MesGeH_3$ (5 mTorr in SF_6, 10 Torr) gave good absorption signals at both 17111.31 and 17118.67 cm^{-1}, clearly indicating the formation of GeH_2.[5] In the absence of added substrate, decay constants of ca. 5×10^4 s^{-1} were obtained. Kinetic experiments were carried out in the normal way, to obtain second order rate constants for reaction of the intermediate with two of the previously used[5] substrate species, Me_3SiH and 1,3-butadiene, using the 17111.31 cm^{-1} monitor. These experiments yielded values of $(8.65 \pm 0.38) \times 10^{-11}$ and $(3.4 \pm 0.2) \times 10^{-10}$ cm^3 $molecule^{-1}$ s^{-1}, respectively. Since these are in satisfactory agreement with those obtained earlier[5] with DMGCP as germylene precursor (see Discussion),

(8) Becerra, R.; Frey, H. M.; Mason, B. P.; Walsh, R.; Gordon, M. S. *J. Chem. Soc., Faraday Trans.* **1995**, *91*, 2723.
(9) Baggott, J. E.; Frey, H. M.; Lightfoot, P. D.; Walsh, R. *J. Phys. Chem.* **1987**, *91*, 3386.
(10) I. W. Carpenter, Ph.D. Thesis, University of Reading, 1996.
(11) Mironov, V. F.; Gar, T. K. *Izv. Akad. Nauk. SSSR, Ser. Khim.* **1966**, 482.
(12) Satgé, J.; Rivière, P. *Bull. Soc. Chim. Fr.* **1966**, 1773.
(13) Rivière, P.; Rivière-Baudet, M.; Castel, A.; Satgé J.; Lavabre, A. *Synth. React. Inorg. Met.-Org. Chem.* **1987**, *17*, 539.
(14) Piper, T. S.; Wilson, M. K. *J. Inorg. Nucl. Chem.* **1957**, *4*, 22.
(15) Brauer, G. *Handbuch der Preparativen Anorganischen Chemie*, Band 2, 3 Auflage; Ferdinand Enke Verlag: New York, 1978.
(16) Lindemann, L. P.; Wilson, M. K. *J. Chem. Phys.* **1954**, *22*, 1723.
(17) Foresman, J. B.; Frisch, A. *Exploring Chemistry with Electronic Structure Methods*, 2nd ed.; Gaussian Inc.: Pittsburgh, 1995.
(18) Curtiss, L. A.; Raghavachari, K.; Trucks, G. W.; Pople, J. A. *J. Chem. Phys.* **1991**, *94*, 7221.
(19) Scott, A. P.; Radom, L. *J. Phys. Chem.* **1996**, *100*, 16502.
(20) Frisch, M. J.; Trucks, G. W.; Schlegel, H. B.; Gill, P. M. W.; Johnson, B. G.; Robb, M. A.; Cheeseman, J. R.; Keith, T.; Petersson, G. A.; Montgomery, J. A.; Raghavachari, K.; Al-Laham, M. A.; Zakrzewski, V. G.; Ortiz, J. V.; Foresman, J. B.; Cioslowski, J.; Stefanov, B. B.; Nanayakkara, A.; Challacombe, M.; Peng, C. Y.; Ayala, P. Y.; Chen, W.; Wong, M. W.; Andres, J. L.; Replogle, E. S.; Gomperts, R.; Martin, R. L.; Fox, D. J.; Binkley, J. S.; Defrees, D. J.; Baker, J.; Stewart, J. P.; Head-Gordon, M.; Gonzales, C.; Pople, J. A. *Gaussian 94*, Revision D.1; Gaussian Inc.: Pittsburgh, 1995.

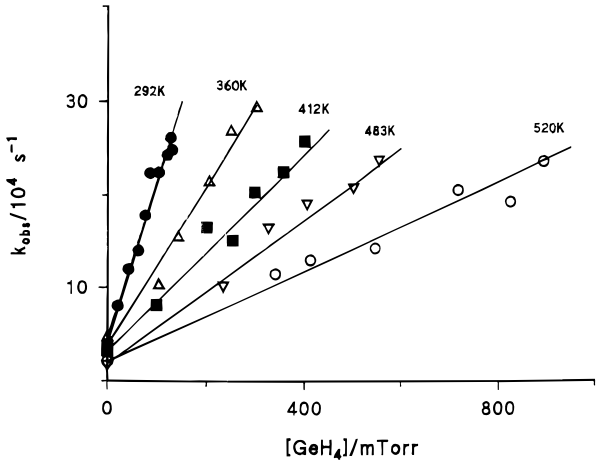

Figure 1. Second-order plots of dependence of k_{obs} on germane pressure in SF_6 (10 Torr) at different temperatures: ●, 292 K; △, 360 K; ■, 412 K; ▽, 483 K; ○, 520 K.

Table 1. Experimental Rate Constants for Reaction 1 at Different Temperatures

T/K	$k(SF_6, 10\ Torr)^a$	$k^{\infty\ a,b}$
292	5.07 ± 0.21	5.5 ± 0.6
360	3.25 ± 0.11	3.9 ± 0.4
412	2.36 ± 0.09	3.1 ± 0.3
483	2.00 ± 0.09	2.8 ± 0.4
520	1.08 ± 0.06	1.95 ± 0.2

[a] Units: 10^{-11} cm^3 molecule^{-1} s^{-1}. [b] Obtained by extrapolation (RRKM assisted; see text).

this provides the desired confirmation for the continued use of DMGCP as GeH_2 precursor.

For the main study, a preliminary check showed that GeH_4 itself was not a source of GeH_2 (GeH_4 did not photodecompose at 193 nm). Checks showed that decay constants for GeH_2 in the presence of GeH_4 were not dependent on the exciplex laser energy or the number of photolysis laser shots. For most experiments five shots of 60 mJ/pulse were used. The DMGCP partial pressure was 3.6 mTorr in most experiments. A series of experiments was carried out at each of five temperatures in the range 292−520 K. The upper temperature limit was determined by the stability of GeH_4 in the reaction vessel. At each temperature and at 10 Torr total pressure, at least five runs at different partial pressures of GeH_4 were carried out. The results of these experiments are shown in Figure 1, which demonstrates the linear dependence of k_{obs} on [GeH_4], as expected for second-order kinetics. The second-order rate constants, obtained by least-squares fitting to these plots, are collected in Table 1. The error limits are single standard deviations and are clearly quite small. Table 1 also includes the values of k^∞, the rate constants at infinite pressure obtained by extrapolation with RRKM theory (see below). These have somewhat larger error limits, because of the uncertainties of the extrapolation. It is clear that the rate constants of each set decrease with temperature, just as has been found[8] for the analogous SiH_2 reaction 2. Arrhenius plots of these data are shown in Figure 2. The data at 10 Torr possibly show some curvature, but the high-pressure limiting data cannot be distinguished from linear within the scatter. The latter give the following Arrhenius equation:

$$\log(k^\infty/\text{cm}^3\ \text{molecule}^{-1}\ \text{s}^{-1}) = (-11.17 \pm 0.10) + (5.18 \pm 0.74\ \text{kJ mol}^{-1})/RT \ln 10$$

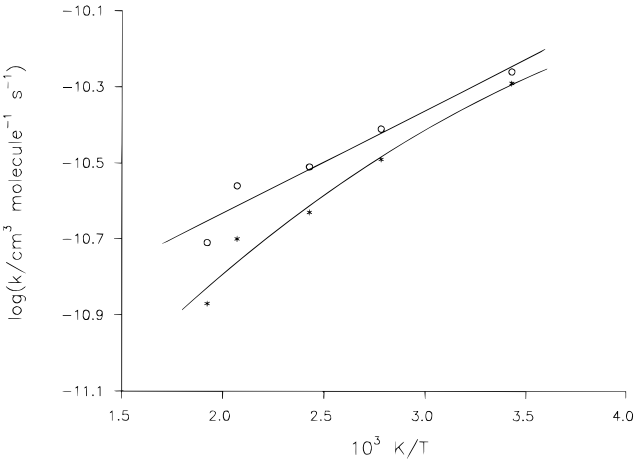

Figure 2. Arrhenius plots of the second-order rate constants for GeH_2 + GeH_4 at different pressures: ∗, 10 Torr; ○, infinite pressure (extrapolated).

In addition to these experiments another set of runs was carried out at each temperature, in which the total pressure (SF_6) was varied in the range 1 to 100 Torr, to test the pressure dependence of the second-order rate constants. The data were obtained in the same way as that at 10 Torr, although since second-order behavior has been established at 10 Torr, only three or four GeH_4 substrate partial pressures were tested at each total pressure. The rate constant for reaction of GeH_2 with precursor (intercept point on the second-order plots) was found to be pressure independent. The pressure range was limited by practical considerations. Above ca. 100 Torr transient signals became too small, and below 1 Torr, pressure measurement uncertainties became significant. The results from these experiments are plotted in Figure 3, which clearly demonstrates the pressure dependence of the rate constants at each temperature. For convenience, log−log plots are used. The uncertainties are not shown in the figures but they are estimated at ca. ±10%.

From examination of Figure 3 several points are evident. Rate constants decrease with increasing temperatures at all pressures. At a given temperature the rate constants increase with increasing pressure, the extent of variation being greatest at the highest temperature. Although the pressure dependence tends toward high pressure limiting values at each temperature, this is only actually reached at 292 K. These effects are characteristic of a third-body mediated association reaction as found previously[8] for reaction 2. For this reason we have carried out RRKM modeling calculations, as described in the next section.

RRKM Calculations. The pressure dependence of an association reaction corresponds exactly to that of the reverse unimolecular dissociation process, providing there are no other perturbing reaction channels. Therefore we have carried out RRKM calculations of the pressure dependence of the digermane unimolecular decomposition, *viz.*

$$Ge_2H_6 \rightarrow GeH_2 + GeH_4 \qquad (-1)$$

The thermal decomposition of digermane is a complex process and its kinetics are highly surface sensitive.[21] There is no published rate data for reaction −1. Therefore we have had to rely on estimation to obtain the required parameters for this reaction. Fortunately this can be done with reasonable reliability and the uncertainties are not large. To obtain the *A* factor, A_{-1},

(21) Emeléus, H. J.; Jellinek, H. H. G. *Trans. Faraday Soc.* **1944**, *40*, 93.

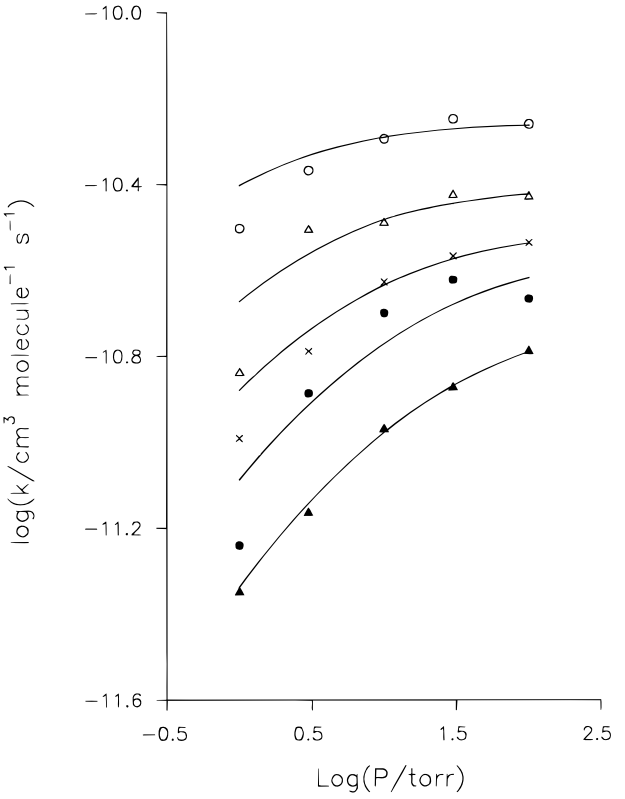

Figure 3. Pressure dependence of second-order rate constants for $GeH_2 + GeH_4$ in the presence of SF_6 at ○, 292 K; △, 360 K; ×, 412 K; ●, 483 K; ▲, 520 K. Curves are RRKM theory fits (see text).

for the reaction, we make use of

$$\Delta S = R \ln(A_{-1}/A_1) \qquad (3)$$

To use eq 3, we need values for ΔS over the temperature range of interest. Although some of the entropy data needed to work this out are available[22−25] it is based on structural information of uncertain reliability. Therefore we have preferred to use the well-known principle of isostructural analogy,[26] using reaction −2, viz., $Si_2H_6 \rightarrow SiH_2 + SiH_4$, as our model. The data are readily available[8] for this reaction and we have subtracted 6.3 J K^{-1} mol^{-1} from $\Delta S(-2)$ to allow for mass and structural differences. The procedure is confirmed by thermodynamic function calculations for Ge_2H_6, GeH_4, and GeH_2 carried out (by us) by using the structures and vibrational wavenumbers generated by the ab initio calculations at the HF level. The resulting values for $\Delta S_{-1,1}$ are shown in Table 2. Using the experimental value for A_1 obtained in this work, we have then calculated the A_{-1} values also shown in Table 2 (care has to be taken in changing from 1 bar reference standard state for entropy to that of 1 molecule cm^{-3} required to use eq 3). We estimate that at most the values of ΔS are uncertain to ±6 J K^{-1} mol^{-1} and the A factors to $10^{\pm 0.3}$. It should be noted that the result of this estimation procedure is to imply non-Arrhenius behavior in the digermane decomposition rate constants, k_{-1}. The change is small over the temperature range 292−520 K, viz. a factor of $10^{0.36}$, but consistent with the variational behavior found by us previously for reaction −2. We cannot say for sure whether this detail is correct since it is within experimental error, but if A_1 is constant, then A_{-1} must decrease slightly over the temperature range of this study.

Table 2. Estimated Thermodynamic and Kinetic Quantities for Digermane Decomposition Reaction (−1,1)

T/K	ΔS/J K^{-1} mol^{-1} [a]	T/K	$\log(A_{-1}/s^{-1})$ [b]
300	131.0	292	14.66
400	130.1	360	14.58
500	128.4	412	14.50
600	127.2	483	14.36
		520	14.30

[a] Estimated; see text. [b] Calculated with eq 3.

Table 3. Molecular and Transition State Parameters for RRKM Calculations for Digermane Decomposition at 298 K

	Ge_2H_6	$Ge_2H_6^{\ddagger}$
$\tilde{\nu}$/cm^{-1}	2150(2)	2150(2)
	2114(2)	2114(1)
	2078(1)	2078(1)
	2070(1)	2070(1)
	898(2)	1500(1)
	875(2)	1000(1)
	765(1)	898(2)
	755(1)	875(2)
	417(2)	765(1)
	407(2)	417(2)
	229(1)	144(1)
	144(1)	100(2)
reaction coordinate	229 cm^{-1}	
I^+/I	1	
path degeneracy	6[a]	
E_o (critical energy)	154.8 kJ mol^{-1} (37.0 kcal mol^{-1})	
collision no. (Z_{LJ})	3.59×10^{-10} cm^3 $molecule^{-1}$ s^{-1} (SF_6)	

[a] This assumes a transition state with loss of symmetry of *one* GeH_3 group, *i.e.*, a bridged structure as found in the ab initio calculation.

The further information required for the RRKM calculations was obtained as follows. The A factor values of Table 2 were used in combination with the molecular wavenumbers of Ge_2H_6[27] to assign wavenumbers of the activated complex at each temperature of the study. In this exercise, $\nu = 229$ cm^{-1} (Ge−Ge stretch) was taken as the reaction coordinate and $\nu = 2114$ cm^{-1} (Ge−H stretch) and 755 cm^{-1} (GeH_3 deformation) were altered to 1500 and 1000 cm^{-1} to reflect the H-bridged nature of the transition state (see ab initio results). The GeH_3 rocking mode wavenumbers, 407 cm^{-1} (2), were varied until a match was achieved with the entropy of activation and the A factor in the usual way.[28,29] The internal rotation was treated as a low wavenumber vibration (144 cm^{-1}) and was not changed in the transition state. Whether the precise values of all wavenumbers are correct is not important provided that the entropy of activation is matched. Because of the apparent decrease in the value of A_{-1} with increasing temperature, which we believe to be correct, we have modified the activated complex (rocking mode wavenumbers) at each temperature to build in variational character, rather than use a temperature-averaged, fixed-wavenumber complex. The details are shown in Tables 3 and 4. We have assumed that the geometry changes in the digermane activated complex do not cause a significant change in the moment of inertia, *i.e.*, that I^+/I is close to unity (our ab initio

(22) Zaitsev, N. M.; Maslov, P. G. *Zh. Prikl. Khim. (Leningrad)* **1972**, *45*, 2184.
(23) Zaitsev, N. M.; Maslov, P. G.; Ivolgin, V. I. *Zh. Prikl. Khim. (Leningrad)* **1974**, *47*, 2020.
(24) Shabur, V. N.; Morozov, V. P. *Teplofiz. Vyz. Temp.* **1978**, *16*, 946.
(25) Shishkin, Yu. A.; Kusner, Yu. S. *Izv. Siberian Otd. Akad. Nauk. SSSR, Ser. Khim.* **1986**, *4*, 11.
(26) Benson, S. W. *Thermochemical Kinetics*, 2nd ed.; Wiley: New York, 1976.
(27) Urban, J.; Schreiner, P. R.; Vacek, G.; Schleyer, P. v. R.; Huang, J. Q.; Leszczynski, J. *Chem. Phys. Lett.* **1997**, *264*, 441.
(28) Robinson, P. J.; Holbrook, K. A. *Unimolecular Reactions*; Wiley: New York, 1972.
(29) Holbrook, K. A.; Pilling, M. J.; Robertson, S. H. *Unimolecular Reactions*, 2nd ed.; Wiley: Chichester, 1996.

Table 4. Temperature-dependent Parameters Used in RRKM Calculations for Digermane Decomposition

	temp/K				
	292	360	412	483	520
TS wavenumber (GeH_3 rock)/cm^{-1}	100(2)	114(2)	128(2)	153(2)	166(2)
10^{10} Z_{LJ}/cm^3 molecule^{-1} s^{-1}	3.59	3.69	3.77	3.87	3.93

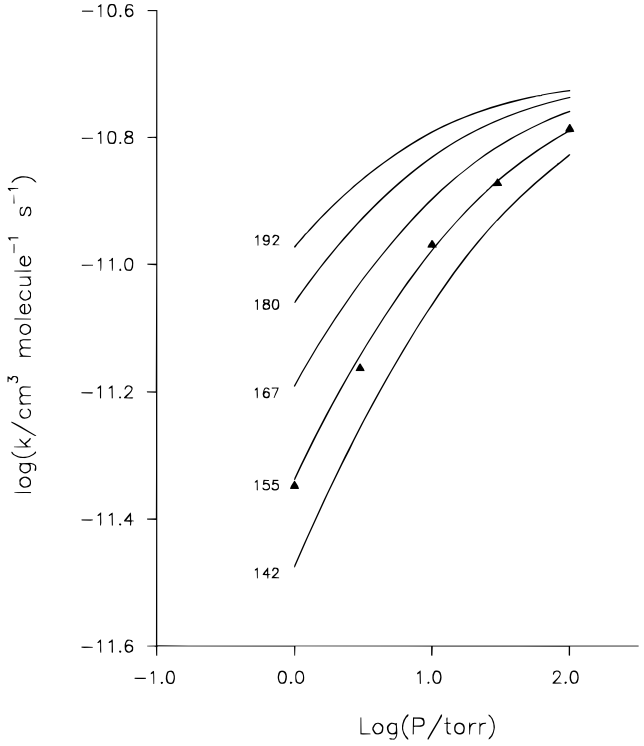

Figure 4. The dependence of RRKM theoretical curves (pressure dependence) on critical energy, E_o/kJ mol^{-1}, for GeH_2 + GeH_4 at 520 K. ▲ indicates experimental data points.

results support this), and that this is valid at all temperatures, so that there are no adiabatic rotational effects (angular momentum conservation problems). The key unknown quantity is the value for the critical (Marcus) energy, E_o, since there has been no previous investigation of this reaction. We have therefore used E_o as a floating parameter in the RRKM calculations themselves.

We have used a weak collisional (stepladder) model for collisional deactivation,[28,29] since there is considerable evidence against the strong collision assumption.[30] We have found previously for SF_6 as the bath gas collision partner values for the average energy removal parameter, $\langle\Delta E\rangle_{down}$, in the range 9.6 to 12.0 kJ mol^{-1}, for reaction systems SiH_2 + SiH_4[8] and SiH_2 + C_2H_4,[31] where falloff characteristics are similar and where the E_o values are well established. The results of our final calculations are shown as full curves in Figure 3. In Figure 4 we show the effect of different choices of E_o within the range 142 to 192 kJ mol^{-1} at 520 K. This clearly demonstrates the sensitivity of the model to changes in E_o. We also varied $\langle\Delta E\rangle_{down}$ but in the end opted for a value of 9.6 kJ mol^{-1} because it better matched the changes in curvatures of the pressure dependence plots with temperature. The matching of the curves with experiment in Figure 3 is generally good and within the scatter of data. The agreement is worst with some, but not all, of the lowest pressure data. Since uncertainties are largest in the data under these conditions we put the differences down to experimental uncertainty. It is worth pointing out that we have used the RRKM theory curves to extrapolate the data to obtain k^∞ values, necessary to provide the required information about the transition state for the reaction. This simply means that we have carried out the series of calculations twice in a cycle to refine the fits. The main outcome of the fitting is the value of 154.8 kJ mol^{-1} for E_o. Uncertainties in this value arise from the data fitting, the collisional efficiency ($\langle\Delta E\rangle_{down}$ = 9.6 kJ mol^{-1} corresponds to $\beta_c \approx 0.7$), and the transition state assignment from the uncertainty in the *A* factors. We estimate these (conservatively) at ±12 kJ mol^{-1}.

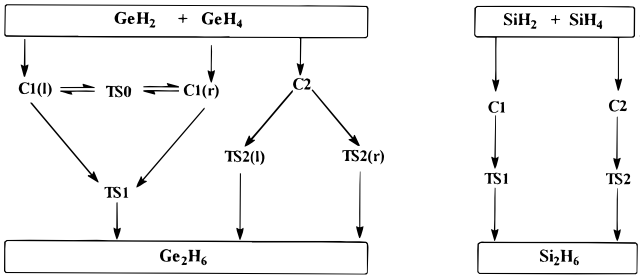

Figure 5. Topology of the potential energy surfaces for the reactions GeH_2 + GeH_4 → Ge_2H_6 and SiH_2 + SiH_4 → Si_2H_6[8] from ab initio MP2/6-311G(d,p) calculations.

Enthalpy of Formation of GeH_2. This may be simply obtained from E_o. Correction for thermal energy at 298 K gives E_a for reaction −1 ($E_a(-1)$) = 158.0 kJ mol^{-1}. Then the enthalpy change, $\Delta H°(-1,1) = 165.7$ kJ mol^{-1}, is obtained via $\Delta H°(-1,1) = E_a(-1) - E_a(1) + RT$. The uncertainty of ±12 kJ mol^{-1} in E_o transfers to $\Delta H°(-1,1)$. When this latter is combined with the literature values[32] of $\Delta H_f^\circ(GeH_4) = 90.4 \pm 2.1$ kJ mol^{-1} and $\Delta H_f^\circ(Ge_2H_6) = 161.9 \pm 1.3$ kJ mol^{-1}, this leads to $\Delta H_f^\circ(GeH_2) = 237.2 \pm 12$ kJ mol^{-1}. The uncertainty comes almost entirely from uncertainties in the RRKM modeling. They would be substantially reduced if a good direct measurement of the activation energy for digermane decomposition, viz. $E_a(-1)$, were available.

Ab Initio Calculations. Apart from the reactants, GeH_2 + GeH_4, and product, Ge_2H_6 itself, five other stationary points have been found on the Ge_2H_6 potential energy surface. These correspond to two local minima, C1 and C2, and three transition states, TS0, TS1, and TS2. The minima represent H-bridged weakly bound complexes with binding energies some 13−18% of that of digermane. Each complex has an associated transition state, TS1 and TS2, linking it to digermane. An additional feature of the complex C1 is its C_1 symmetry, and existence as left (C1l) or right (C1r) handed forms, which are separated by the very low rotational transition state TS0. A similar situation was found for transition state TS2. It also has C_1 symmetry, and possesses left (TS2l) and right (TS2r) handed forms divided by a low rotational maximum. The linking of pathways through these stationary points on the Ge_2H_6 potential energy surface is shown in the topology diagram of Figure 5. This picture was verified by the IRC calculations. The IRC trajectory starting from TS2 (TS2l or TS2r) ended in the forward direction at the digermane minimum and in the backward direction at C2. The IRC trajectory starting from TS1 in the forward direction also ended at digermane, but in the back direction it finished at TS0. This is due to the fact that the quasi-Newton method used for

(30) Hippler, H.; Troe, J. In *Advances in Gas-Phase Photochemistry and Kinetics*; Ashfold, M. N. R., Baggott, J. E., Eds.; Royal Society of Chemistry: London, 1989; Vol. 2, Chapter 5, p 209.

(31) Al-Rubaiey, N.; Walsh, R. *J. Phys. Chem.* **1994**, *98*, 5303.

(32) Gunn, S. R.; Green, L. G. *J. Phys. Chem.* **1961**, *65*, 779.

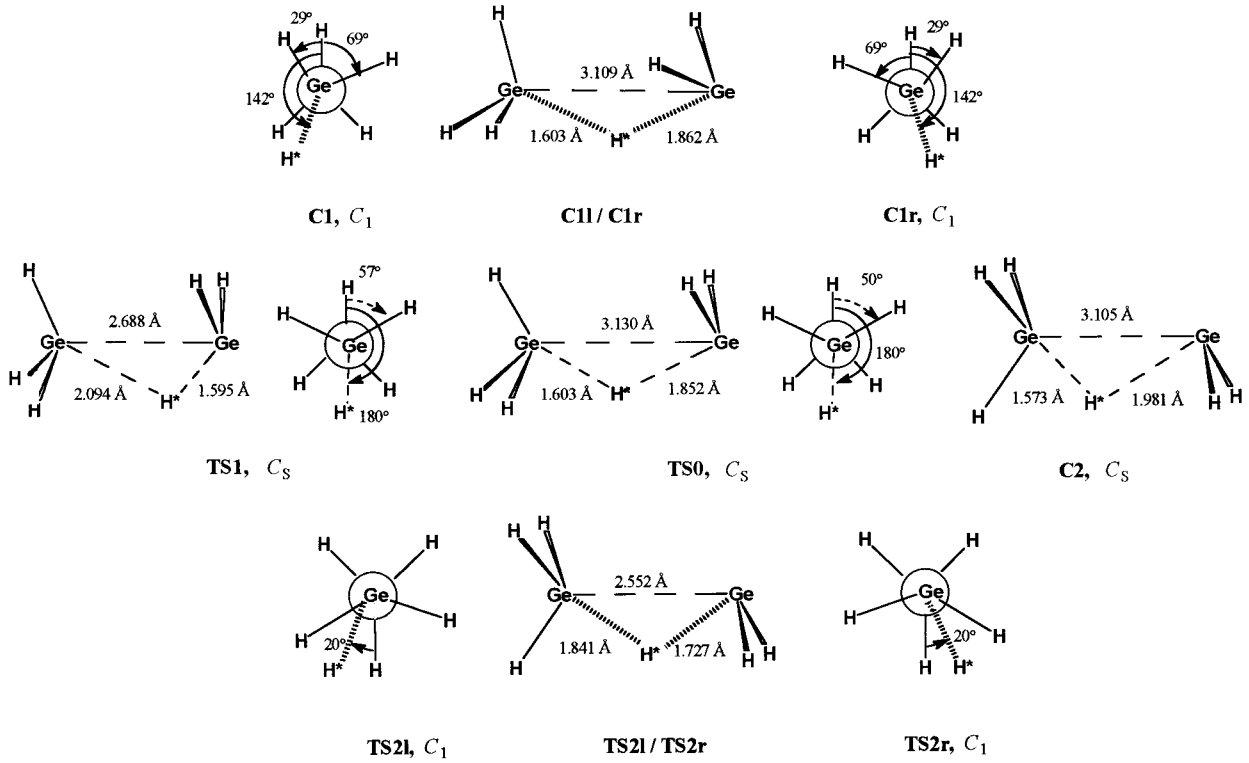

Figure 6. Ab initio MP2/6-311G(d,p) calculated geometries of local minimum structures and transition states on the $GeH_2 + GeH_4 \rightarrow Ge_2H_6$ energy surface. Point groups are given beside each structure (see text and Figure 5 for location on the surface). The migrating H atoms are marked with an asterisk.

the IRC calculation retains the C_s symmetry throughout the optimization process. However, calculations of the IRC reaction paths from TS0 show that it connects C1l and C1r. Despite the complexity of these right- and left-handed species, implying a bifurcation in each reaction pathway, the passage through C1 to digermane involves an inversion of configuration of the forming GeH_3 group, whereas that through C2 does not. This is just as for the equivalent pathways on the Si_2H_6 surface.[8] The reaction pathways over the Ge_2H_6 surface are compared with those over the Si_2H_6 surface in Figure 5.

The salient features of these structures are shown in Figure 6. For GeH_2, the bond length and angle are calculated to be 1.582 Å and 93.1°, respectively, while for GeH_4 the calculated bond length is 1.531 Å. For digermane, the calculated Ge−Ge and Ge−H bond lengths are 2.452 and 1.534 Å, respectively, while the H−Ge−Ge bond angle is 109.8°. For the isolated molecules these calculated geometries are in good agreement with experimental values[33] and previous high level ab initio calculations.[34]

The Ge_2H_6 potential energy surface is quite similar to that of Si_2H_6,[8] except that in the latter case all the stationary point species, i.e., both complexes and transition states, are of C_s symmetry. In this respect the two complexes with associated transition states correspond to two different approach geometries of GeH_2 with GeH_4. In the first (C1 and TS1) the GeH_2 approaches with its H atoms facing and lone pair orbital away from GeH_4, *i.e.*, a syn configuration, while in the second, GeH_2 has its lone pair angled toward GeH_4 and its H atoms away, *i.e.*, an anti configuration. An analysis of structures C1 and C2 in Figure 6 reveals that in both complexes the migrating atom (H*) is closer to the initial monogermane atom Ge(1) than the germylene atom Ge(2). Thus in C1 the distances Ge(1)−H* and Ge(2)−H* are 1.603 and 1.862 Å, respectively, while in C2 they are 1.573 and 1.981 Å, respectively. This indicates that H-atom transfer is not very advanced in either case. This contrasts with complexes on the Si_2H_6 surface.[8] In the analogue to C1, Si(1)−H* and Si(2)−H* are 2.046 and 1.525 Å, respectively, thus showing much more significant H-transfer. For C2, Si(1)−H* and Si(2)−H* are 1.548 and 1.760 Å, respectively, more akin to the Ge_2H_6 analogue with much less H-atom transfer.

The energies associated with all the stationary point species are shown in Table 5. It can be seen that energetically the C1 + TS1 pathway is favored over C2 + TS2 at each level of the calculation and that these conclusions are not altered by inclusion of zero-point energy effects. Both pathways involve complexes with low barriers to rearrangement to Ge_2H_6. These barriers are quite small and the transition states lie below the starting $GeH_2 + GeH_4$ energy except for the G2 calculation for TS2 where the energy is marginally higher (by 0.7 kJ mol^{-1}). The very small barrier for interconversion of C1l and C1r, corresponding to transition state TS0, also disappears in the G2 calculation, although we note that the harmonic approximation for vibrations is not very good for loose structures such as the complexes and transition states found here. When thermal energies are also added to the electronic energies calculated here (G2 level), the overall enthalpy change at 298 K is calculated to be −180.6 kJ mol^{-1}, which compares reasonably well with the RRKM value, derived in this study.

In the computational study of $SiH_2 + SiH_4$ some polarity of the intermediate complexes and transition states was noted.[8] In this study calculated dipole moments of complexes and transition states (Table 5) vary from 1.4 to 2.3 D. Mullikan population

(33) Graner, G.; Hirota, E.; Iijima, T.; Kuchitsu, K.; Ramsay, D. A.; Vogt, J.; Vogt, N. *Structure Data of Free Polyatomic Molecules*; Landolt-Börnstein New Series; Kuchitsu, K., Ed.; Springer-Verlag: Berlin, 1998; Group II, Vol. 25A.

(34) Leszczynski, J.; Huang, J. Q.; Schreiner, P. R.; Vacek, G.; Kapp, J.; Schleyer, P. von R.; Schaefer, H. F. *Chem. Phys. Lett.* **1995**, *244*, 252.

Table 5. *Ab Initio* Calculated Energies (E/hartree, ΔE/kJ mol^{-1}) and Dipole Moments (D) of the Stationary Points of the $GeH_2 + GeH_4 \rightarrow Ge_2H_6$ Reaction Potential Energy Surface

		MP2/6-311G(d,p)[a]			G2//MP2/6-311G(d,p)		G2[c]		
species	PG	E	ΔE[b]	ΔE + ZPE	E	ΔE[b]	E	ΔE[b]	dipole
GeH_2	C_{2v}	−2076.52048			−2076.57028		−2076.57212		0.01
GeH_4	T_d	−2077.75259			−2077.79718		−2077.79890		0.00
Ge_2H_6	S_6	−4154.34661	−193.1	−178.9	−4154.43476	−176.7	−4154.43827	−176.5	0.00
Compl C1	C_1	−4154.28600	−33.9	−23.0	−4154.37822	−25.3			2.26
TS0(Rot)	C_s	−4154.28561	−32.9	−22.7	−4154.37807	−24.9			2.33
TS1	C_s	−4154.28101	−20.8	−13.8	−4154.37489	−16.6			1.37
Compl C2	C_s	−4154.28335	−27.0	−17.4	−4154.37603	−19.6			2.06
TS2	C_1	−4154.27346	−1.0	−7.3	−4154.36832	0.7			1.36

[a] MP2/6-311G(d,p)//MP2/6-311G(d,p) level. [b] Relative to isolated $GeH_2 + GeH_4$. [c] G2 method with standard choice of geometry and frequencies.

Table 6. Measured Rate Constants (k/10^{-11} cm^3 molecule^{-1} s^{-1} at Room Temperature[a]) for Reactions of GeH_2 from Different Sources

substrate	DMGCP[b]	$PhGeH_3$[b]	$MesGeH_3$[c]
Me_3SiH	8.18 ± 0.14	2.81 ± 0.26	8.65 ± 0.38
1,3-C_4H_6	30.3 ± 1.2	15.1 ± 0.9	34 ± 2

[a] 292−294 K. [b] Reference 5. [c] This work.

analysis shows that the absolute charges of the reacting fragments, viz., $GeH_2 + GeH_4$ in the complexes and TS2, and $GeH_3 + GeH_3$ in TS1, are in the range 0.126−0.189 au, with GeH_2 bearing the negative charge. These are higher than the calculated[8] values (0.069−0.112 au) for the respective local minima and TS's in the $SiH_2 + SiH_4$ reaction. This indicates an increased polarity in the Ge−H insertion process.

Discussion

General Comments and Rate Constant Comparisons. As a preliminary to the main study we sought further validation of our use of DMGCP as a GeH_2 precursor suitable for kinetic studies. The results obtained with the new precursor, $MesGeH_3$, are compared with those obtained previously with DMGCP and $PhGeH_3$ as precursors, in Table 6. It can be seen clearly that, within experimental error, the rate constants obtained with the transients from $MesGeH_3$ and DMGCP are in agreement with one another, whereas they differ from those obtained with $PhGeH_3$ as precursor. This provides strong support for our previous arguments[5,6] in favor of the rate constants obtained with DMGCP as being correct for the GeH_2 species. We have offered an explanation as to why the apparent rate constants for GeH_2 from $PhGeH_3$ might be in error,[5] which we do not repeat here. However, it should be pointed out that $MesGeH_3$, also an aromatic precursor, cannot be subject to the same problem.

The main experimental purpose of this study was to measure rate constants, including their temperature and pressure dependence, for the reaction of $GeH_2 + GeH_4$ for the first time. This has been achieved and the rate constants, just like those for $SiH_2 + SiH_4$,[8] have been found to decrease with temperature and increase with pressure. At the high-pressure limit, the reaction has an activation energy of −5.2 kJ mol^{-1}, comparable to, but more negative than, that of $SiH_2 + SiH_4$[8] (−3.3 kJ mol^{-1}) and less negative than that of $GeH_2 + Et_3GeH$[6] (−10.6 kJ mol^{-1}). If the magnitude of the rate constant at infinite pressure is compared to an estimated Lennard-Jones collision number at 292 K (3.3×10^{-10} cm^3 molecule^{-1} s^{-1}) it can be seen that the reaction occurs with a collisional efficiency of 0.17. The lower collisional efficiency of reaction 1 compared to its silicon analogue, reaction 2, is also reflected in the lower A factor, viz., $10^{-11.17}$ cm^3 molecule^{-1} s^{-1} for A_1 compared to $10^{-9.91}$ cm^3 molecule^{-1} s^{-1} for A_2.

Table 7. Comparison of Gas-phase Rate Constants (k/cm^3 molecule^{-1} s^{-1}) for Si−H Insertion (SiH_2) and Ge−H Insertion (GeH_2)

	298 K		600 K	
reaction	k^∞	k_{rel}(per X−H)	k^∞	k_{rel}(per X−H)
$SiH_2 + SiH_4$	4.6×10^{-10} [a]	1	2.4×10^{-10} [a]	1
$SiH_2 + Me_3SiH$	2.5×10^{-10} [b]	2.2	1.40×10^{-10} [b]	2.3
$GeH_2 + GeH_4$	5.5×10^{-11} [c]	0.12(1)[e]	1.92×10^{-11} [c]	0.080(1)[e]
$GeH_2 + Et_3GeH$	2.7×10^{-10} [d]	2.3(19.6)[e]	3.1×10^{-11} [d]	0.52(6.5)[e]

[a] Reference 8. [b] References 35 and 36. [c] This work. [d] Reference 6. [e] With reaction 1 as reference.

It is interesting to compare SiH_2 insertion selectivities into Si−H bonds with GeH_2 insertion selectivities into Ge−H bonds. These may be calculated from currently known rate constants and are shown in Table 7. It is immediately apparent that GeH_2 is a more selective species than SiH_2 in these processes. Thus alkyl (3 methyls) substitution at Si enhances the SiH_2 insertion rate by only a factor of 2.2 almost independent of temperature, whereas alkyl (3 ethyls) substitution at Ge enhances the GeH_2 insertion rate by a factor of 20 at 298 K and 6.5 at 600 K. The factor changes with temperature because the reactions slow to a different extent. These greater selectivities (and lower rate constants) for GeH_2 can be understood in terms of a mechanism via an intermediate complex (see below).

RRKM Calculations. There is no previous RRKM calculation for reaction 1 or its reverse (−1). The calculations carried out here cannot be judged by their fit to the experiment, since this has been carefully optimized by adjustment of E_o, the critical energy for reverse dissociation of digermane. Thus we comment here on the magnitude of some of the input parameters and how they compare with those for the similar calculations for the decomposition of disilane.[8] The pressure dependence (degree of falloff) is most sensitive to the magnitudes of the A factor and the critical energy. The A factor for decomposition of Ge_2H_6, A_{-1}, is determined by the entropy change and A_1 and should not be in error by more than $10^{\pm 0.3}$. It is interesting to note that the A_{-1} values of Table 2 span the range $10^{14.3}$−$10^{14.7}$ s^{-1} while those for A_{-2}, the A factor for decomposition of Si_2H_6, cover the range $10^{15.5}$−$10^{16.4}$ s^{-1}. This arises mainly because for the forward insertion reactions A_1 is ca. $10^{1.3}$ smaller than A_2. Thus the transition state for digermane decomposition is significantly tighter than that for disilane decomposition. There must be more effective H bridging in the activated complex for reaction 1 than for reaction 2. The fact that $A_{-1} < A_{-2}$ means that for equal values of E_o and temperature, (−1) should show less falloff than (−2). However, from the experimental results the extent of falloff at a given temperature is, if anything, greater for (−1) than for (−2). This can only be put down to a significantly lower E_o value for (−1) than (−2). The conse-

quences of weak collisional effects, although not negligible, are unlikely to differ significantly between the two systems. The dependence of the falloff on $E_o(-1)$ is seen directly in Figure 4, at 520 K, the temperature of greatest sensitivity. This enables us to fix E_o with reasonable confidence at 155 kJ mol^{-1} (*cf.* $E_o(-2) \approx 217$ kJ mol^{-1}). We have treated E_o as a fixed quantity, even though the evidence of this and earlier work[8] favors a variational transition state. It is hard to estimate the error arising from this assumption, but we note that in our study of $SiH_2 + SiH_4$ the change in E_o was only -7 kJ mol^{-1} between 296 and 658 K, and in the present study the variational character is less. We doubt that this can be a serious source of error.

Uncertainties over the precise efficiency of SF_6 in the weak collisional model have already been argued to be small. Last we consider the question of chemical perturbations. The most likely seems (to us) to be the possibility of the side reaction:

$$Ge_2H_6 \rightarrow H_3GeGeH + H_2 \qquad (4)$$

This is based on analogous arguments for Si_2H_6.[8] However, if this process were a serious perturbation, it would lead to a leveling out of the k_1 pressure dependence curves at higher temperatures and lower pressures. There is no evidence for this and therefore we infer that reaction 4 or another potential decomposition route of Ge_2H_6, or indeed a direct metathesis reaction of $GeH_2 + GeH_4$ to other products, cannot be important.

Potential Energy Surface and the Nature of the Insertion Reaction. The ab initio calculations performed in this work represent an extension of those carried out on the equivalent Si_2H_6 system.[8] The only previous calculations on the Ge_2H_6 system were those of Trinquier,[7] which were at the lower SCF/ECP level of theory. However, the main findings were similar to those of this work, viz., the existence of two intermediate complexes of similar geometry to C1 and C2, with the syn form energetically preferred over the anti form. The point of Trinquier's work[7] was to demonstrate that H-bridged structures such as C1 increase in stability relative to the stable M_2H_6 (C_{3v} form), as M increases in atomic number down Group 14 of the periodic table. At the higher levels of theory of this and previous work,[8] this finding is still born out for Si_2H_6 (bridged form unstable by 184.5 kJ mol^{-1}) and Ge_2H_6 (bridged form unstable by 151.4 kJ mol^{-1}). Relative to the dissociated fragments, however, $H_3Si\cdot\cdot H\cdot\cdot SiH_2$ (LM1) is stable by 51.5 kJ mol^{-1}, while $H_3Ge\cdot\cdot H\cdot\cdot GeH_2$ (C1) is only stable by 25 kJ mol^{-1}, which appears to be against the earlier trend.[7]

For the complex C1, the departure from the more symmetrical C_s to C_1 structure with its right- and left-handed forms is puzzling. This was not found by Trinquier[7] for the Ge_2H_6 species, but was for the equivalent Sn_2H_6 and Pb_2H_6 species. The rotational barriers in the normal M_2H_6 decrease systematically from C_2H_6 (12 kJ mol^{-1}) to Si_2H_6 (5 kJ mol^{-1}) to Ge_2H_6 (ca. 3 kJ mol^{-1}).[27] This is readily accounted for by the reduction in M−H bond interactions as the M−M bond length increases. Thus for the H-bonded complexes one might expect a greater likelihood for internal rotation barriers in Si_2H_6 species than the Ge_2H_6 species, rather than the other way round as appears to be the case. Clearly this problem is more subtle than this argument suggests. One should be cautious in trying to draw strict conclusions about some of these subtle structural points because the region of the potential surface where the minima are located is rather flat and some of the structural features might disappear at even higher levels of calculation.

One of the motivations for the present calculations was to see whether and to what extent they could offer supporting evidence for the kinetic findings. The existence of these complexes provides just such evidence. The presence of weakly bound complexes for the Si−H insertion reactions of SiH_2 and other silylenes has been shown to account for the kinetics in those cases.[8,36,37] The existence of a structural restriction in the form of a secondary barrier, below the threshold energy of $GeH_2 + GeH_4$, is sufficient to create a bottleneck on the Gibbs energy surface. The location of such a bottleneck will depend on the total system energy (and therefore temperature). This will not only give rise to a negative activation energy, but also explain the variational behavior of the transition state. The same feature of the surface also offers a semiquantitative explanation for differences between germylene and silylene insertion reactions. If the secondary barriers are too far below threshold, then their influence on the kinetics will be minimal. This is probably the case for $SiH_2 + SiH_4$, where the rates are virtually collisional and encounter controlled. For $GeH_2 + GeH_4$ the secondary barrier (TS1) is much nearer to the threshold energy (-17 kJ mol^{-1} compared to -48 kJ mol^{-1} for the Si case). This suggests a greater influence of the secondary bottleneck, which will become more important at higher temperatures. This should lead to slower rates for GeH_2 insertion than for SiH_2 insertion. It is interesting also to note that, for the $GeH_2 + GeH_4$ insertion via the *anti*-H-bridged complex C2, the secondary barrier TS2 is just above the threshold. Since the structure is fairly tight, this secondary bottleneck will almost certainly prevent insertion via this pathway. This situation corresponds to an overall reaction steric factor significantly below unity since it means the elimination of one orientation of approach of GeH_2 to GeH_4. This situation is not the case for the $SiH_2 + SiH_4$ reaction, and may go some way toward explaining why the *A* factor in the $GeH_2 + GeH_4$ reaction is less than that for $SiH_2 + SiH_4$. It could also explain the enhanced alkyl substituent effect in the substrate ($GeH_2 + Et_3GeH$ case), since alkyl groups are thought to act by lowering the secondary barrier (at least in silylene insertion reactions[36,37]). If the secondary barrier is exerting more of an effect in the $GeH_2 + GeH_4$ insertion case then the effects of alkyl substitution will be more marked than in the analogous Si−H insertion reactions. Thus the ab initio calculations offer a good explanation for the main kinetic features of $GeH_2 + GeH_4$ insertion reaction, and of the GeH_2 insertions into Ge−H bonds in general.

Enthalpy of Formation and DSSE of GeH_2. The value for $\Delta H_f^\circ(GeH_2)$ of 237 ± 12 kJ mol^{-1} is the most secure so far obtained from kinetic considerations. Previously[38,39] we had estimated a value of 238 ± 12 kJ mol^{-1} based on untested assumptions about the kinetics of Ge_2H_6 pyrolysis, using the published rates of Emeleus and Jellinek[21] (but with a different mechanism). Although this earlier estimate is almost identical to the value found here, it was much less securely based. The present value is also more certain than the figure of 255 ± 42 kJ mol^{-1} estimated by Newman et al.[3] from the kinetics of GeH_4 pyrolysis. The only other experimental value, of >248 kJ mol^{-1} (more probably 258 kJ mol^{-1}), comes from Berkowitz and coworkers[40] and was obtained from photoionization threshold measurements. The agreement with our result is tolerable.

(35) Carpenter, I. W.; Walsh, R. Unpublished results (see ref 36).
(36) Becerra, R.; Walsh, R. in *Research in Chemical Kinetics*; Compton, R. G., Hancock, G., Eds.; Elsevier: Amsterdam, 1995; Vol. 3, p 263.
(37) Baggott, J. E.; Blitz, M. A.; Frey, H. M.; Lightfoot, P. D.; Walsh, R. *J. Am. Chem. Soc.* **1990**, *112*, 8337.
(38) Almond, M. J.; Doncaster, A. M.; Noble, P. N.; Walsh, R. *J. Am. Chem. Soc.* **1982**, *104*, 4717.
(39) Noble, P. N.; Walsh, R. *Int. J. Chem. Kinet.* **1983**, *15*, 547.
(40) Ruscic, B.; Schwartz, M.; Berkowitz, J. *J. Chem. Phys.* **1990**, *92*, 1865.

Theoretical calculations by Grev and colleagues[41] give a value of 250 kJ mol^{-1} in close agreement with our theoretical calcultaions which imply a value of 252 kJ mol^{-1}.

The DSSE (divalent state stabilization energy) is a useful index of reactivity for silylenes[42−45] and its value for GeH_2 may be deduced from the data obtained here. For GeH_2 it is defined as follows:

$$\mathrm{DSSE}(GeH_2) = D(H_3Ge{-}H) - D(H_2Ge{-}H)$$
$$= 2\Delta H_f^{\circ}(GeH_3) - \Delta H_f^{\circ}(GeH_4) - \Delta H_f^{\circ}(GeH_2)$$

For $\Delta H_f^{\circ}(GeH_3)$ we use a value of 223 kJ mol^{-1}. The value obtained by Noble and Walsh[39] has been increased by 5 kJ mol^{-1} in accordance with the generally accepted view[46] that the original assumptions of the method gave slight underestimates. $\Delta H_f^{\circ}(GeH_4) = 90.4$ kJ mol^{-1}.[32] If we use $\Delta H_f^{\circ}(GeH_2) = 237$ kJ mol^{-1} this yields $\mathrm{DSSE}(GeH_2) = 119$ kJ mol^{-1}. Despite uncertainties probably amounting to ± 20 kJ mol^{-1}, this value is still greater than the figure of 94 ± 4 for $\mathrm{DSSE}(SiH_2)$.[44] Grev[45] has reached similar conclusions. Thus the divalent state stabilization increases as we proceed down group XIV, a phenomenon that has long been known and often discussed in other chemical contexts as the "Inert Pair Effect".[47]

Acknowledgment. We thank the following: (i) the Royal Society of Great Britain for support under its joint project scheme with States of the Former Soviet Union (Grant P851); (ii) the Russian Foundation for Basic Research (Grants N 95-07-20201 and N 97-03-33757); (iii) the CACR Computer Center at the Zelinsky Institute for computer time on the SGI Power Challenge L: and (iv) the Direccion General de Investigacion Cientifica y Technica (DGICYT), Spain, for support to R.B. under project PB94-0218-CO2-01.

JA983223M

(41) Karolczak, J.; Harper, W. W.; Grev, R. S.; Clouthier, D. J. *J. Chem. Phys.* **1995**, *103*, 2839.

(42) Walsh, R. *Pure Appl. Chem.* **1987**, *59*, 69.

(43) Walsh, R. Derivation of thermodynamic quantities from kinetic measurements in gas-phase silane chemistry. In *Energetics of Organometallic Species*; Martinho-Simôes, J. A., Ed; NATO-ASI Ser. C.; Kluwer: Dordrecht, 1992; Vol. 367, Chapter 11, p 171.

(44) Becerra, R.; Walsh, R. Thermochemistry. In *The Chemistry of Organosilicon Compounds*; Rappoport, Z., Apeloig, Y., Eds.; Wiley: Chichester, 1998; Vol. 2, Chapter 4, p 153.

(45) Grev, R. *Adv. Organomet. Chem.* **1991**, *33*, 125.

(46) Berkovitz, J.; Ellison, G. B.; Gutman, D. *J. Phys. Chem.* **1994**, *98*, 2744.

(47) Dasent, W. E. *Nonexistent Compounds*; Arnold: London, 1965; Chapter 5, p 77.